


Metasurfaces for de Broglie waves

Wan-yue Xiao^{1,2} and Cheng-ping Huang^{1,*}

¹*Department of Physics, Nanjing Tech University, Nanjing 211816, China*

²*Department of Physics, City University of Hong Kong, Kowloon, Hong Kong 999077, China*

 (Received 26 April 2021; revised 1 November 2021; accepted 13 December 2021; published 23 December 2021)

Metasurfaces have been employed to control the electromagnetic and acoustic waves. We suggest that the quantum particles can be manipulated with a de Broglie wave metasurface. The effect was achieved by using the dielectric films milled with subwavelength slits, which behave as the quantum meta-atoms with an effective potential energy. The calculations show that $\sim 100\%$ transmission of de Broglie waves may appear in certain conditions. Moreover, by tuning the effective potential of the slits, a full 360° coverage of transmission phase is attainable. With a carefully designed annular metasurface, highly efficient and subwavelength focusing of de Broglie waves has been theoretically demonstrated. Our work may render a way to manipulate quantum particles.

DOI: [10.1103/PhysRevB.104.245429](https://doi.org/10.1103/PhysRevB.104.245429)

I. INTRODUCTION

Interaction of waves with artificial materials has been an important topic in physics for decades. The research on this topic has led to a variety of interesting physical effects and various valuable applications. On the one hand, when the wave propagates along the periodically modulated structure, the bandgap effect may be induced because of the Bragg reflection. Some well-known examples include the propagation of de Broglie waves in semiconductor superlattices, light waves in photonic crystals, and elastic waves in phononic crystals [1–6]. On the other hand, when the wave propagates perpendicular to the modulated structure, especially the quasi-two-dimensional array of subwavelength components (called the *metasurfaces*), anomalous transmission effects will be present. For example, metal films milled with periodic apertures can support enhanced optical transmission, beaming of light, and polarization rotation, etc. [7–10]. With the phase gradient along the metasurface, for another example, anomalous reflection/refraction, focusing, and holographic display, etc., can be achieved [11–16].

As we know, progress from optical to electron microscopes represents a significant step toward modern microscopic imaging techniques, where de Broglie waves or quantum particles play a crucial role. Existing ways to manipulate quantum particles are based on the electric field [17,18], magnetic field [19,20], and light field [21,22], which usually need bulky and complicated instruments. Although the metasurfaces have been explored extensively to control the wave front of electromagnetic and acoustic waves [23–25], no such manmade materials have been reported for de Broglie or matter waves. In addition to the shorter wavelength, this may be limited by the transmission property of matter waves. Generally, the transmission of matter waves through small apertures is dominated by tunneling and is negligible. Al-

though the transmission may be increased by introducing the surface potential well and surface matter waves [26–28], the resulting system will become complicated, and the transmission peak is extremely narrow. On the other hand, in optical metasurfaces consisting of metallic nano-antennas, light can penetrate the metal and drive the plasmonic resonance, thus inducing radiation of light with phase shift covering the full 2π range [12–14]. A similar effect is not available for matter waves.

In this paper, we propose that a metasurface for de Broglie waves can be constructed which may control the transmission amplitude and phase simultaneously. The metasurface is composed of a single-layer dielectric film tailored with subwavelength slits of designed sizes, acting as meta-atoms with effective and adjustable potential energy that can perturb the motion of particles. We suggest that, at the Rayleigh anomaly or waveguide resonances, $\sim 100\%$ transmission of de Broglie waves can be achieved. Moreover, by tuning the effective potential energy of meta-atoms, the full 2π coverage of the transmission phase is attainable. Based on these results, we show that highly efficient and subwavelength focusing of de Broglie waves can be obtained with an annular gradient metasurface. In this paper, we show the possibility of controlling matter waves with planar microstructured insulator materials (instead of semiconductor materials), which may be valuable for the microscopic imaging and lithography, etc.

II. RESULTS AND DISCUSSIONS

Figure 1 presents the schematic view of the quasi-two-dimensional structure (the side length is much larger than the wavelength of de Broglie waves), consisting of a single-layer dielectric film tailored with subwavelength slits of equal spacing d and gradient or homogeneous slit width a_i ($i = 1 - n$). The dielectric film, with a thickness of h , is assumed to be in vacuum. The matter waves (e.g., the electron waves), with the de Broglie wavelength λ , normally impinge on the structure along the $-z$ direction. The dielectric film will block the

*cphuang@njtech.edu.cn

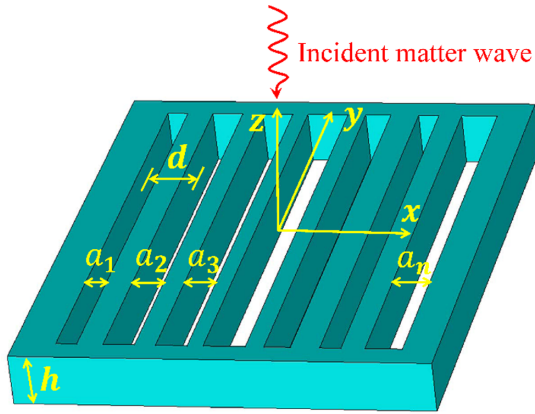


FIG. 1. Schematic view of the de Broglie wave metasurface. The dielectric film of thickness h is tailored with subwavelength slits of equal spacing d (the distance between the centers of the slits) and gradient or homogeneous slit width a_i ($i = 1 - n$). The plane matter waves (with the wavelength λ) are normally incident on the metasurface along the $-z$ direction.

matter waves, and the subwavelength slits function as the channels or new sources of matter waves, giving rise to emission with certain amplitude and phase. If the amplitude and phase of matter waves at the exits of slits can be engineered properly, the wavefront could be controlled at will.

A. Properties of single slits

The issue involves the interaction between particles and the dielectric medium. Generally, the particles, e.g., the high-energy incident electrons, can penetrate the dielectric medium, leading to various effects such as electron scattering, phonon excitation, x-ray radiation, etc. Here, the situation is different, as discussed below. We take the normal incidence of electrons at a flat vacuum/dielectric interface as an example. The matter waves studied here are of low energy, and the de Broglie wavelength (~ 100 nm) is much larger than the atomic lattice constant. Thus, the waves experience an averaged response near the dielectric surface, where the dielectric is characterized by a mean inner potential V_I ($V_I \sim +10\text{--}20$ V) [29–31]. Because of the normal wave vector mismatching at the interface, the waves are usually reflected and/or transmitted. The transmission of matter waves into the dielectric is [32]

$$\frac{\psi_T}{\psi_I} = \frac{2}{1 + \sqrt{1 + \frac{V_I e}{E_0}}}, \quad (1)$$

where e and E_0 are the charge (absolute value) and energy of the electrons, respectively. For the low-energy electrons with $E_0 \ll V_I e$ (or $\lambda \gg h/\sqrt{2mV_I e} \sim 0.3$ nm), the transmission will be very small ($\psi_T/\psi_I \approx 1\%$ for the wavelength considered here). The transmission further degenerates when the incident angle is increased. Therefore, the wave function in the dielectric medium can be neglected, like the case that the dielectric has an infinite potential or a light wave impinges on a metal film.

The behavior of matter waves in the subwavelength slits (sandwiched between two dielectric walls) is crucial for

determining the transmission properties of the system. To understand this point, one should solve the Schrödinger equation in the slit and use the boundary conditions on the slit walls (where the wave function is set as zero, according to the above discussion). Note that, for the larger film thickness, one need only to consider the fundamental waveguide mode in the slits; the higher-order modes decay rapidly and can be neglected. Thus, the wave function of the fundamental slit mode has the following format: $\psi_{\text{slit}} = f(z) \cos(\pi x/a)$, where $x \in [-a/2, a/2]$. By substituting this format of wave function into the Schrödinger equation, one can obtain

$$-\frac{\hbar^2}{2m} \frac{\partial^2 \psi_{\text{slit}}}{\partial z^2} + \frac{\hbar^2 \pi^2}{2ma^2} \psi_{\text{slit}} = E \psi_{\text{slit}}, \quad (2)$$

where m and E are the mass and energy of the particles.

Equation (2) means that the subwavelength slits act as quantum meta-atoms which present an effective potential energy $U_{\text{eff}} = \hbar^2 \pi^2 / 2ma^2$. Correspondingly, the propagation of matter waves in the slits turns into the motion of particles in the meta-atoms. Just like the role of permittivity/permeability in the electromagnetic Helmholtz equation, the effective potential energy U_{eff} in the Schrödinger equation will influence the wave propagation behavior as well. By using Eq. (2), the propagation constant of the slit mode can be determined as $q_0 = \sqrt{2m(E - U_{\text{eff}})}/\hbar$. Obviously, when the energy of particles E is larger than the effective potential energy U_{eff} , the matter wave propagates in the slits, which may cause an efficient transmission (otherwise, the wave is evanescent, and a weak tunneling process will take place). The balance between E and U_{eff} gives rise to a cutoff wavelength for the fundamental mode (FM) $\lambda_c = 2a$ [33], where $\lambda = h/\sqrt{2mE}$ is the wavelength of matter waves in free space. Because the effective potential energy U_{eff} is inversely proportional to the square of the slit width (the smaller the slit width a , the larger the U_{eff}), a variation of slit width will change U_{eff} significantly. Consequently, the propagation constant q_0 of waves and the motion of particles in the slits can be modified. This gives us the possibility to manipulate the matter waves with an array of meta-atoms (in the propagating cases).

B. Transmission amplitude and phase of homogeneous slit arrays

A simple case is that the metasurface is degenerated into a periodic structure with homogeneous slit width $a_i = a$. Such a case can be treated theoretically with the modal expansion method, like that used in the electromagnetic diffraction problems [34,35]. The zero-order transmission coefficient of the de Broglie waves can be derived as [see Appendix]

$$T_0 = \frac{\tau_1 \tau_2 e^{iq_0 h}}{1 - \rho^2 e^{2iq_0 h}}. \quad (3)$$

Equation (3) suggests that the structured film behaves like an effective Fabry-Perot cavity for the matter waves, with the two cavity boundaries defined by the upper and lower film interfaces. Here, $\tau_1 = 2\theta_0/(1 + \theta)$ and $\tau_2 = 2/(1 + \theta)$ are the effective transmission coefficients at the two boundaries; $\rho = (1 - \theta)/(1 + \theta)$ is the internal effective reflection coefficient of the cavity; $\theta = (2k_0 a/q_0 d) \sum_n u_n X_n^2$ and $\theta_0 = (2k_0 a/q_0 d) X_0^2$, where $u_n = \sqrt{1 - G_n^2/k_0^2}$, $X_n =$

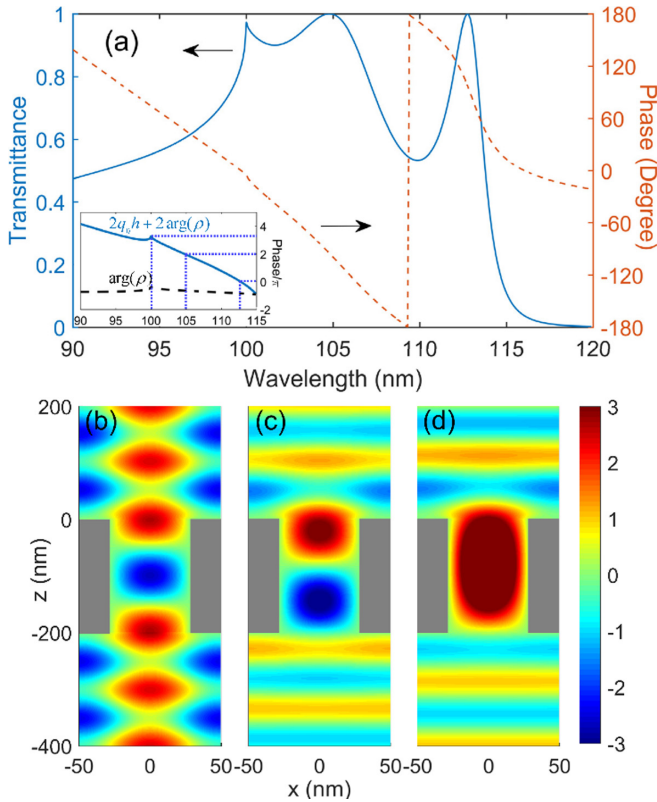


FIG. 2. (a) Calculated transmittance and transmission phase of the periodically structured film. The inset shows the phase shift of the slit mode in a round trip (solid line) and at the openings (dash line) as a function of wavelength, where the vertical dotted lines denote the three peak wavelengths. (b)–(d) Near-field distributions (normalized to the amplitude of incident wave) in the xz plane of a unit cell at the peak wavelength (b) 100 nm, (c) 105 nm, and (d) 113 nm. Here, $d = 100$ nm, $a = 58$ nm, and $h = 200$ nm.

$(1/a) \int_{-a/2}^{a/2} \cos(\pi x/a) e^{\pm i G_n x} dx$ is the mode-overlapping integral, k_0 is the wave vector in free space, and $G_n = 2\pi n/d$ is the reciprocal lattice vector. With Eq. (3), the transmittance $t_0 = |T_0|^2$ and phase $\varphi_t = \arg(T_0)$ of matter waves can be obtained easily. Note that, in Eq. (3), T_0 is closely correlated with the slit propagation constant q_0 and thus with the effective potential energy U_{eff} or the slit width a . Indeed, this provides the space for controlling the transmission amplitude and phase of the matter waves.

For the structures with subwavelength period and narrow slits ($\lambda > d \geq 2a$), the slits work in the cutoff region, and the transmittance was found to be very low. However, for the structures with subwavelength period but wide slits ($2a > \lambda > d$), the slit mode is propagating, and efficient transmission can be achieved. To demonstrate this point, the structural parameters were set as follows: the period $d = 100$ nm, the width of the slits $a = 58$ nm ($a > d/2$), and the film thickness $h = 200$ nm. The transmittance and phase as a function of wavelength are calculated and shown in Fig. 2(a). Remarkably, three transmission peaks locating around the wavelengths 100, 105, and 113 nm can be found, with the transmission efficiency very close to unity. The total bandwidth of the three peaks is ~ 20 nm (relative band width

is $\sim 20\%$), much larger than that achieved with the surface waves [19]. The $\sim 100\%$ transmission of matter waves through dielectric films with wider slits (without the surface potential wells) provides an efficient way for manipulating the quantum particles. When the wavelength approaches the cutoff wavelength (116 nm), the transmission of matter waves will decrease rapidly. In addition, the calculation also shows that the transmission phase (the dash line) will vary with the wavelength almost linearly.

It is well known that the excitation of surface modes, e.g., the surface plasmon polariton and surface matter waves, is a major mechanism responsible for the enhanced transmission [7,26]. However, here, the surface matter waves are not present. To understand the mechanism of efficient transmission, the near-field distributions for the three transmission peaks are calculated and plotted in Figs. 2(b)–2(d). The results show that the slit mode exhibits a stationarylike pattern, and its amplitude is greatly enhanced at the transmission peaks. Thus, the enhanced transmission might be related to the waveguide resonance. According to Eq. (3), the condition for waveguide resonances can be expressed as $2q_0 h + 2 \arg(\rho) = 2\pi m$ [m is an integer and $\arg(\rho)$ represents the phase shift of slit mode at the upper or lower openings]. Our calculation, as shown in inset of Fig. 2(a), indicates that the peaks at the wavelengths 113 and 105 nm correspond to the zero ($m = 0$)- and first ($m = 1$)-order waveguide resonances, respectively. However, the peak at the wavelength 100 nm, just matching the lattice period d , cannot be attributed simply to the waveguide mode. In this case, the first-order diffraction modes of the matter waves are tangent to the film surface, thus corresponding to the Rayleigh anomaly. As shown in the following, this peak always exists in the transmission spectra with the peak position independent of the slit sizes ($\lambda = d < 2a$), different from other transmission peaks.

Figures 3(a) and 3(b) show the transmission efficiency and phase for different slit width a , where the lattice constant and film thickness were fixed as $d = 100$ nm and $h = 300$ nm, and the slit width a was varied from 59 to 85 nm. Figure 3(a) indicates that, for each slit width a , multiple transmission peaks are present. Generally, the positions of these peaks rely on the value of a , corresponding to the resonances of waveguide mode. Importantly, for all cases, a common transmission peak with the efficiency approaching 100% can be found at the wavelength of the Rayleigh anomaly ($\lambda = d = 100$ nm). On the other hand, Fig. 3(b) shows that, for each slit width, the transmission phase varies with the wavelength almost linearly. For a given wavelength, the phase will increase with the slit width gradually. For example, at the Rayleigh anomaly, a phase increment $\sim 60^\circ$ can be achieved when the slit width a increases from 59 nm to 62, 66, 70, 76, and 85 nm (when the wavelength deviates from the Rayleigh anomaly, the transmittance can still maintain at a high level, and a similar phase increment can be kept). Therefore, by varying the slit width, a full 360° phase control is attainable.

C. Focusing of matter waves with gradient slit arrays

By utilizing the above transmission characters at the Rayleigh anomaly, i.e., the insensitivity of transmission amplitude and sensitivity of transmission phase to the slit width,

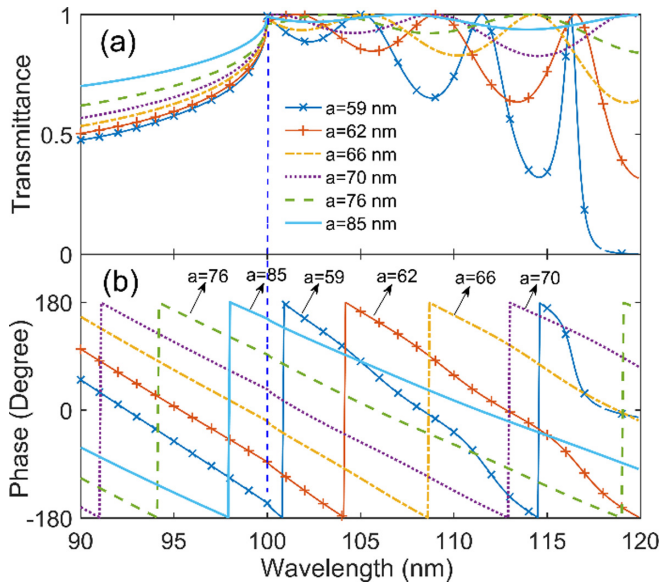


FIG. 3. (a) Transmittance and (b) phase as a function of wavelength for periodic structure with different slit widths a . Here, $d = 100$ nm and $h = 300$ nm. The vertical dash line corresponds to the Rayleigh anomaly.

efficient wavefront shaping of matter waves can be realized. For instance, if the dielectric film is structured with super unit cells, each consisting of six slits of the same spacing but gradient slit width (as used in Fig. 3), one can obtain a de Broglie wave metasurface which owns a constant phase gradient along the surface. Such a metasurface can be applied to realize the bending of matter waves.

Now we will design a flat metalens based on the gradient metasurface to focus the matter waves. The metalens is constructed by a dielectric film tailored with concentric annular slits, which have the same slit spacing d but gradient slit width a_n along the radial direction (note that a two-dimensional array of rectangular holes of gradient size a_x can also work, where $a_x \ll a_y$ and $d_x < d_y$). The schematic view of the metalens and the related coordinate system are shown in Fig. 4(a).

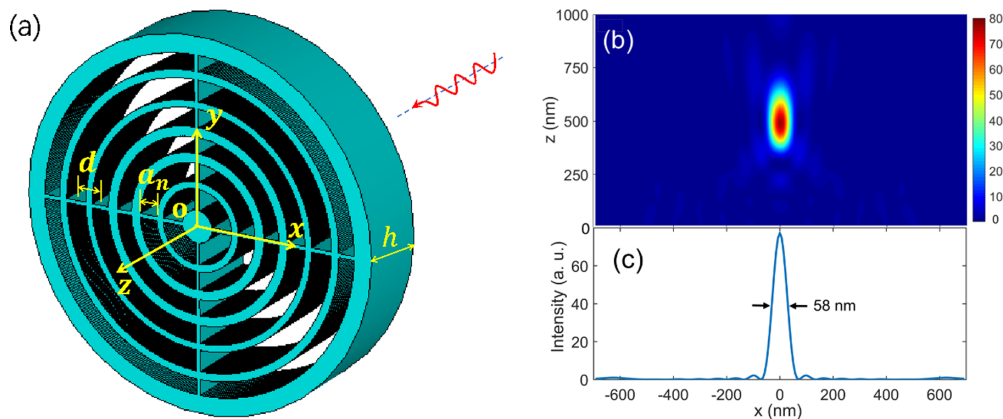


FIG. 4. (a) Schematic view of the matter wave metalens. The matter wave is normally incident on the metalens along the z axis. (b) Distribution of the intensity of matter waves at the xz plane (the color scale is of arbitrary units). (c) The intensity of matter waves along the x axis at the focal plane. Here, the spacing of annular slits is $d = 100$ nm, the film thickness is $h = 300$ nm, and the wavelength of matter waves is fixed as 100 nm.

For simplicity, here, only six annular slits in the film are considered, where the spacing of slits and film thickness are fixed as $d = 100$ nm and $h = 300$ nm, respectively. The matter waves with the wavelength λ are normally incident on the metalens along the $+z$ direction. To function as a flat lens with the focal length f , the phase profile at the metalens surface needs to follow

$$\varphi_n = \varphi_1 - \frac{2\pi}{\lambda} (\sqrt{r_n^2 + f^2} - \sqrt{r_1^2 + f^2}), \quad (4)$$

where φ_n ($n = 1-6$ denotes the n th annular slit counted from the center of the metalens) is the transmission phase at the opening of the n th slit and $r_n = nd$ represents the central radius of the n th slit.

For the incident scalar matter waves, the concentric annular slits of equal spacing feel like the one-dimensional slits in the radial direction. Moreover, due to the excitation of the localized waveguide mode, the transmission phase is largely governed by the individual slits. This enables us to determine the width of each slit based on the previous calculation [Eq. (3)] and the required phase profile at the metalens [Eq. (4)]. Here, we set the incident wavelength as $\lambda = d = 100$ nm and aim at focusing with the focal length of $f = 500$ nm. The slit widths a_n and transmission phase φ_n for each annular slit that comprise the flat metalens are thus determined, as listed in Table I. Because of the Rayleigh anomaly, the transmittance of each slit is around unity. Consequently, each annular slit acts as the source of wavelets, with the transmitted matter wave function at the slit opening written simply as $\psi_n^{z=0} = e^{i\varphi_n}$. The superposition of wavelets emitted by the annular slits gives rise to the focusing wave fields of the metalens.

Based on Kirchhoff's diffraction formula [36], the total wave function passing through the annular metalens can be obtained as

$$\psi_r(x, y, z) = \frac{1}{2i\lambda} \sum_{n=1}^6 e^{i\varphi_n} \int_{\sigma_n} \frac{e^{ik_0 s_n}}{s_n} \left[1 + \frac{z}{s_n} \left(1 - \frac{1}{ik_0 s_n} \right) \right] d\sigma_n, \quad (5)$$

TABLE I. The slit widths a_n and transmission phase φ_n for each annular slit shown in Fig. 4(a). Here, n denotes the n th slit counted from the center of the metalens.

n	a_n (nm)	φ_n (deg)
1	80	122
2	68	10
3	60	-130
4	68	10
5	80	122
6	60	-130

where s_n is the distance between the observation point (x, y, z) and the source point P $(r \cos \alpha, r \sin \alpha, 0)$ at the opening of the n th annular slit, r is the distance between the point P and the coordinate origin O $(nd - a_n/2 \leq r \leq nd + a_n/2)$, α is the angle between the line OP and the x axis, and σ_n denotes the integral area covering the whole area of the n th annular slit. With the transmission phase φ_n and slit width a_n listed in Table I, the wave function and the intensity of matter waves at arbitrary observation point (x, y, z) have been numerically calculated by using Eq. (5). Figure 4(b) maps the distribution of the intensity of matter wave in the xz plane. Clearly, a focusing of matter waves at the focal length of 500 nm with high intensity has been suggested. In addition, Fig. 4(c) plots the intensity of matter waves along the x axis at the focal plane ($z = 500$ nm). The full width at half maximum (FWHM) of the focal intensity is ~ 58 nm, which is smaller than the wavelength (100 nm) but slightly larger than the half wavelength of the incident wave, indicating that the focusing is diffraction limited. The results show that highly efficient focusing of matter waves can be achieved with a flat metalens. It should be noticed that our theoretical treatment is based on the single-particle approximation, and the space charge effect was not accounted. The approximation holds for the electron beams with low current densities. When the current density is increased, the repulsion of electrons will modify the diffraction pattern, and the FWHM of the focal intensity will be enlarged. A similar effect also exists in the conventional electron lenses.

III. CONCLUSIONS

In summary, metasurfaces for the de Broglie waves have been proposed and studied. We showed that, at the waveguide resonances or Rayleigh anomaly, $\sim 100\%$ transmission of matter waves through the subwavelength slits can be achieved. Moreover, the subwavelength slits may function as quantum meta-atoms, where the particles will feel an effective potential energy dominated by the slit width. Thus, by varying the effective potential energy, a full coverage of 360° of the transmission phase is attainable. Employing an annular gradient metasurface, highly efficient and subwavelength focusing of matter waves has been demonstrated theoretically. The wavefront shaping of matter waves with flat metasurfaces may be valuable for subwavelength resolution imaging, lithography, and holography, etc. Our results could be extended to the region of shorter de Broglie wavelength, such as several

nanometers, but this may raise challenges for nanofabrication techniques.

ACKNOWLEDGMENTS

This paper was supported by the National Natural Science Foundation of China (Grant No. 12174193).

APPENDIX

We assume that the low-energy particles, with the de Broglie wavelength much larger than the atomic lattice constant, are incident normally upon the freestanding dielectric film that is milled with the subwavelength slits. The spatial potential experienced by the particles is set as zero except for the dielectric region. As discussed previously, the particles will be prevented from entering the dielectric medium (where the wave function is ~ 0), equivalent to an infinite potential for the dielectric. Moreover, the incident particles (e.g., electrons) have a low density; thus, the space charge effect can be neglected, and the problem is simplified as the single-particle one. For a given particle energy E , the wave functions in the free space are governed by the single-particle stationary Schrödinger equation:

$$\left(\nabla^2 + \frac{2mE}{\hbar^2}\right)\psi(x, z) = 0. \quad (\text{A1})$$

As is well known, Eq. (A1) is like the Helmholtz equation of the time-harmonic electromagnetic fields.

When the metasurface is degenerated into a periodic structure (see Fig. 5), the wave functions of Eq. (A1) in regions I, II, and III can be expressed with the modal expansion method as (ignoring the time-harmonic items)

$$\begin{aligned} \psi^{\text{I}}(x, z) &= e^{-ik_0z} + \sum_{n=0}^{\pm\infty} R_n e^{i(G_n x + u_n k_0 z)}, \\ \psi^{\text{II}}(x, z) &= (A_0 e^{iq_0 z} + B_0 e^{-iq_0 z}) C_0(x), \\ \psi^{\text{III}}(x, z) &= \sum_{n=0}^{\pm\infty} T_n e^{i[G_n x - u_n k_0(z+h)]}. \end{aligned} \quad (\text{A2})$$

Here, $k_0 = \sqrt{2mE}/\hbar = 2\pi/\lambda$ is the wave vector in free space (λ is the de Broglie wavelength), $G_n = 2\pi n/d$ (n is an integer) is the reciprocal lattice vector, and $u_n = \sqrt{1 - G_n^2/k_0^2}$; R_n and T_n are, respectively, the reflection and transmission coefficients corresponding to the n th-order diffraction modes

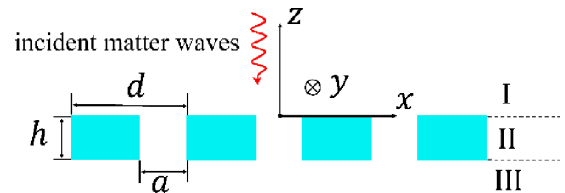


FIG. 5. Schematic view of the de Broglie wave metasurface in the periodic case, where the subwavelength slits are cut in the film with homogeneous slit width $a_i = a$. The h and d denote the thickness and period of the slits, respectively. The plane matter waves (with the wavelength λ) are normally incident on the metasurface along the $-z$ direction.

(for subwavelength structure, only the zero-order mode is propagating, and the other modes are all evanescent); A_0 and B_0 are, respectively, the amplitudes of the backward and forward waves in the slits, $q_0 = \sqrt{k_0^2 - (\pi/a)^2}$ is the propagation constant of the fundamental slit mode, and $C_0(x) = \cos(\pi x/a)$ ($|x| \leq a/2$) or $C_0(x) = 0$ ($a/2 < |x| < d/2$) (the single-mode approximation is used in the slits, as the FM will play a dominant role in our case).

The wave functions of de Broglie waves satisfy the boundary conditions at the two horizontal film interfaces. One boundary condition is the continuity of wave functions in a lattice period ($|x| \leq d/2$):

$$\begin{aligned}\psi^I(x, 0^+) &= \psi^{II}(x, 0^-), \\ \psi^{II}(x, -h^+) &= \psi^{III}(x, -h^-).\end{aligned}\quad (\text{A3})$$

The other boundary condition is the continuity of gradient of wave functions at the slit openings ($|x| \leq a/2$):

$$\begin{aligned}\nabla_z \psi^I(x, 0^+) &= \nabla_z \psi^{II}(x, 0^-), \\ \nabla_z \psi^{II}(x, -h^+) &= \nabla_z \psi^{III}(x, -h^-).\end{aligned}\quad (\text{A4})$$

The boundary conditions can be treated using the following way. We replace ψ [Eq. (A2)] into Eq. (A3), multiply both sides of Eq. (A3) with $e^{-iG_m x}$, and perform the integral over one period. Likewise, we replace ψ in Eq. (A4), multiply both sides of Eq. (A4) with $\cos(\pi x/a)$, and perform the integral over the slit width. By utilizing the orthogonal conditions $(1/d) \int_{-d/2}^{d/2} e^{iG_n x} e^{-iG_m x} dx = \delta_{mn}$ and $(2/a) \int_{-a/2}^{a/2} \cos^2(\pi x/a) dx = 1$, we have the following equations:

$$R_m = w(A_0 + B_0)X_m - \delta_{m0}, \quad (\text{A5})$$

$$T_m = w(A_0 e^{-iq_0 h} + B_0 e^{iq_0 h})X_m, \quad (\text{A6})$$

$$A_0 - B_0 = \frac{2k_0}{q_0} \left(-X_0 + \sum_{m=0}^{\pm\infty} R_m u_m X_m \right), \quad (\text{A7})$$

$$A_0 e^{-iq_0 h} - B_0 e^{iq_0 h} = -\frac{2k_0}{q_0} \sum_{m=0}^{\pm\infty} T_m u_m X_m. \quad (\text{A8})$$

Here, $w = a/d$ is the duty cycle of the slits, and X_m represents the overlapping integral between the fundamental slit mode and surface diffraction modes at the openings of the slits:

$$X_m = \frac{1}{a} \int_{-a/2}^{a/2} \cos \frac{\pi x}{a} e^{\pm iG_m x} dx. \quad (\text{A9})$$

By using Eqs. (A5)–(A8), one can obtain A_0 , B_0 , R_m , and T_m , thus determining the wave functions in the space [Eq. (A2)]. The zero-order transmission coefficient of the system, in which we are mostly interested, can be derived as

$$T_0 = \frac{\tau_1 \tau_2 e^{iq_0 h}}{1 - \rho^2 e^{2iq_0 h}}, \quad (\text{A10})$$

where $\tau_1 = 2\theta_0/(1 + \theta)$ and $\tau_2 = 2/(1 + \theta)$ are the effective transmission coefficients at the upper and lower film interfaces, respectively; $\rho = (1 - \theta)/(1 + \theta)$ is the effective reflection coefficient in the cavity defined by the dielectric film; $\theta_0 = (2k_0 a/q_0 d)X_0^2$ and $\theta = (2k_0 a/q_0 d)\sum_n u_n X_n^2$. With Eq. (A10), the amplitude and phase of zero-order transmission of de Broglie waves can be obtained.

-
- [1] B. Saha, A. Shakouri, and T. D. Sands, Rocksalt nitride metal/semiconductor superlattices: A new class of artificially structured materials, *Appl. Phys. Rev.* **5**, 021101 (2018).
- [2] A. Apostolakis and M. F. Pereira, Controlling the harmonic conversion efficiency in semiconductor superlattices by interface roughness design, *AIP Advances* **9**, 015022 (2019).
- [3] R. K. Cersonsky, J. Antonaglia, B. D. Dice, and S. C. Glotzer, The diversity of three-dimensional photonic crystals, *Nat. Commun.* **12**, 2543 (2021).
- [4] Y. Liu, H. Wang, J. Ho, R. C. Ng, R. J. Ng, V. H. Hall-Chen, E. H. Koay, Z. Dong, H. Liu, and C.-W. Qiu, Structural color three-dimensional printing by shrinking photonic crystals, *Nat. Commun.* **10**, 4340 (2019).
- [5] Y.-F. Wang, Y.-Z. Wang, B. Wu, W. Chen, and Y.-S. Wang, Tunable and active phononic crystals and metamaterials, *Appl. Mech. Rev.* **72**, 040801 (2020).
- [6] Y. Jin, B. Djafari-Rouhani, and D. Torrent, Gradient index phononic crystals and metamaterials, *Nanophotonics* **8**, 685 (2019).
- [7] T. W. Ebbesen, H. J. Lezec, H. Ghaemi, T. Thio, and P. Wolff, Extraordinary optical transmission through sub-wavelength hole arrays, *Nature (London)* **391**, 667 (1998).
- [8] H. J. Lezec, A. Degiron, E. Devaux, R. A. Linke, L. Martin-Moreno, F. J. Garcia-Vidal, and T. W. Ebbesen, Beaming light from a subwavelength aperture, *Science* **297**, 820 (2002).
- [9] C. Genet and T. W. Ebbesen, Light in tiny holes, *Nature (London)* **445**, 39 (2007).
- [10] C. P. Huang, J. Y. Hua, Y. Zhang, and X. G. Yin, Transmissive and efficient 90° polarization rotation with a single-layer plasmonic structure, *Appl. Phys. Express* **10**, 112201 (2017).
- [11] J. Wang and Y. Jiang, Gradient metasurface for four-direction anomalous reflection in terahertz, *Opt. Commun.* **416**, 125 (2018).
- [12] N. Yu, P. Genevet, M. A. Kats, F. Aieta, J.-P. Tetienne, F. Capasso, and Z. Gaburro, Light propagation with phase discontinuities: Generalized laws of reflection and refraction, *Science* **334**, 333 (2011).
- [13] S. Sun, K.-Y. Yang, C.-M. Wang, T.-K. Juan, W. T. Chen, C. Y. Liao, Q. He, S. Xiao, W.-T. Kung, and G.-Y. Guo, High-efficiency broadband anomalous reflection by gradient meta-surfaces, *Nano Lett.* **12**, 6223 (2012).
- [14] F. Qin, L. Ding, L. Zhang, F. Monticone, C. C. Chum, J. Deng, S. Mei, Y. Li, J. Teng, and M. Hong, Hybrid bilayer plasmonic metasurface efficiently manipulates visible light, *Sci. Adv.* **2**, e1501168 (2016).

- [15] G. Yoon, K. Kim, D. Huh, H. Lee, and J. Rho, Single-step manufacturing of hierarchical dielectric metalens in the visible, *Nat. Commun.* **11**, 2268 (2020).
- [16] H. Ren, X. Fang, J. Jang, J. Bürger, J. Rho, and S. A. Maier, Complex-amplitude metasurface-based orbital angular momentum holography in momentum space, *Nat. Nanotechnol.* **15**, 948 (2020).
- [17] K. Yang, W. Paul, S.-H. Phark, P. Willke, Y. Bae, T. Choi, T. Esat, A. Ardavan, A. J. Heinrich, and C. P. Lutz, Coherent spin manipulation of individual atoms on a surface, *Science* **366**, 509 (2019).
- [18] J. E. Palmer and S. D. Hogan, Electric Rydberg-Atom Interferometry, *Phys. Rev. Lett.* **122**, 250404 (2019).
- [19] J. R. Gardner, E. M. Anciaux, and M. G. Raizen, Neutral atom imaging using a pulsed electromagnetic lens, *J. Chem. Phys.* **146**, 081102 (2017).
- [20] W.-Y. Chang and F.-R. Chen, Wide-range tunable magnetic lens for tabletop electron microscope, *Ultramicroscopy* **171**, 139 (2016).
- [21] M. Norcia, A. Young, and A. Kaufman, Microscopic Control and Detection of Ultracold Strontium in Optical-Tweezer Arrays, *Phys. Rev. X* **8**, 041054 (2018).
- [22] C. Diboune, N. Zahzam, Y. Bidel, M. Cadoret, and A. Bresson, Multi-line fiber laser system for cesium and rubidium atom interferometry, *Opt. Express* **25**, 16898 (2017).
- [23] S. Xiao, T. Wang, T. Liu, C. Zhou, X. Jiang, and J. Zhang, Active metamaterials and metadevices: A review, *J. Phys. D Appl. Phys.* **53**, 503002 (2020).
- [24] B. Sain, C. Meier, and T. Zentgraf, Nonlinear optics in all-dielectric nanoantennas and metasurfaces: A review, *Adv. Photonics* **1**, 024002 (2019).
- [25] B. Assouar, B. Liang, Y. Wu, Y. Li, J.-C. Cheng, and Y. Jing, Acoustic metasurfaces, *Nat. Rev. Mater.* **3**, 460 (2018).
- [26] E. Moreno, A. Fernández-Domínguez, J. I. Cirac, F. García-Vidal, and L. Martín-Moreno, Resonant Transmission of Cold Atoms through Subwavelength Apertures, *Phys. Rev. Lett.* **95**, 170406 (2005).
- [27] A. Fernández-Domínguez, E. Moreno, L. Martín-Moreno, and F. Garcia-Vidal, Beaming matter waves from a subwavelength aperture, *Phys. Rev. A* **74**, 021601(R) (2006).
- [28] A. Fernandez-Dominguez, D. Martin-Cano, E. Moreno, L. Martin-Moreno, and F. Garcia-Vidal, Resonant transmission and beaming of cold atoms assisted by surface matter waves, *Phys. Rev. A* **78**, 023614 (2008).
- [29] A. Sanchez and M. A. Ochoa, Calculation of mean inner potential, *J. Phys. C Solid State Phys.* **18**, 33 (1985).
- [30] D. K. Saldin and J. C. H. Spence, On the mean inner potential in high- and low-energy electron diffraction, *Ultramicroscopy* **55**, 397 (1994).
- [31] H. Y. Sun, Z. W. Mao, T. W. Zhang, L. Han, T. T. Zhang, X. B. Cai, X. Guo, Y. F. Li, Y. P. Zang, W. Guo, J. H. Song, D. X. Ji, C. Y. Gu, C. Tang, Z. B. Gu, N. Wang, Y. Zhu, D. G. Schlom, Y. F. Nie, and X. Q. Pan, Chemically specific termination control of oxide interfaces via layer-by-layer mean inner potential engineering, *Nat. Commun.* **9**, 2965 (2018).
- [32] A. Ichimiya and P. I. Cohen, *Reflection High-Energy Electron Diffraction* (Cambridge University Press, Cambridge, 2004).
- [33] There are significant differences for the propagation behavior of acoustic, electromagnetic, and matter waves in the slits or square holes. For acoustic waves, the FM has no cutoff in both slits and holes; for electromagnetic waves, the FM has a cutoff in the hole but the p-polarized FM has no cutoff in the slit; and for the matter waves, the FM has a cutoff for both holes and slits.
- [34] P. Sheng, R. Stepleman, and P. Sanda, Exact eigenfunctions for square-wave gratings: Application to diffraction and surface-plasmon calculations, *Phys. Rev. B* **26**, 2907 (1982).
- [35] F. J. Garcia-Vidal, L. Martin-Moreno, T. Ebbesen, and L. Kuipers, Light passing through subwavelength apertures, *Rev. Mod. Phys.* **82**, 729 (2010).
- [36] M. Born and E. Wolf, *Principles of Optics Electromagnetic Theory of Propagation, Interference and Diffraction of Light* (Cambridge University Press, Cambridge, England, 1999).